Development and Control of a Flexible Actuation-Based Delta Robot

Yasiru Fernando
School of Engineering and Technology,
Asian Institute of Technology,
Pathum Thani, Thailand
yasiruf@yahoo.co.uk

Manukid Parnichkun
School of Engineering and Technology,
Asian Institute of Technology,
Pathum Thani, Thailand
manukid@ait.asia

IECON 2022 – 48th Annual Conference of the IEEE Industrial Electronics Society | 978-1-6654-8025-3/22/$31.00 ©2022 IEEE | DOI: 10.1109/IECON49645.2022.9968565

***Abstract*— Delta robots are a popular type of robot used in industry for fast actuation whereas soft robotics is an emerging branch of robotics that aims to develop robots with flexible bodies. This research aims to develop a Delta Robot with flexible actuation to further the research carried out for soft robotic development. Most soft robots in literature utilize bending type actuators. The Reverse Pneumatic Artificial Muscle (RPAM) was used in this study as the type of flexible actuator which is ideal for extension-based applications which is necessary for Delta Robot-like behaviour. The RPAM was convenient to develop with latex rubber tubes and inextensible fiber wrappings in a double helical pattern. This configuration of fiber wrapping restricts radial expansion of the flexible tube and allows the actuator to have a high length to pressure increment ratio. Thereby, RPAMs provide a near linear relationship between pressure and strain as compared to other types of flexible actuators in literature. The robot developed in this study utilizes three RPAM actuators powered by compressed air. With such a configuration, the robot was expected to operate in a hemispherical working space. The robot developed achieved a hemispherical working space of radius 12.37cm and variation angle of 31º. PID control was used to regulate the pressure within the actuators. Through the actuation sequences of the solenoid valves, the robot end effector position was controlled with respect to the pressure of each actuator. Through the use of a Look-Up Table and interpolation, the robot can be commanded to move to the desired position in the working volume to successfully perform pick and place operations.**

Keywords*— *Flexible Actuator, Delta Robot, Reverse Pneumatic Artificial Muscle.

I. INTRODUCTION

Delta robots are fast with great precision and are typically utilized in the pharmaceutical and electronic industry. The linkages for Delta robots are configured parallelly which provide the dexterity to perform the fast pick and place tasks. In the recent past, researchers have strived to incorporate softer materials for robot bodies paving the way for Soft Robotics. Soft robots are the type of robots that utilize soft and compliant materials along with suitable actuation techniques to provide delicate motions and manipulations. Soft robots are known to be adaptations of nature's most versatile creatures. Due to the use of power sources such as pneumatics, controlling the soft robot is more difficult. Furthermore, they require specialized methods of feedback along with advanced control mechanisms.

Many types of soft robotic actuators that operate by bending [1] or changing it's length [2][3] have been designed by researchers. Skorina et al., [4] developed a Reverse Pneumatic Artificial Muscle (RPAM) using silicone with fiber reinforcements. This type of actuator was combined in parallel configuration to develop a parallel manipulator [5]. Hawke et al., [6] developed a similar type of actuator with rubber tubing and inextensible thread as fiber reinforcement. This actuator was able to achieve 300% strain with a near linear relationship between pressure and length change.

Control of soft robotic actuators is challenging. Electronic pressure regulators [7], fluidic drive cylinders [1] and solenoid valves [8] are types of hardware that are generally used to control pressure within the soft actuators.

II. KINEMATIC MODEL

The kinematic model of the robot was formulated to represent the dynamic behavior of the system. Unlike traditional robots, the kinematics require the mapping of configuration space parameters with actuator space and task space [9] as shown in figure 1.

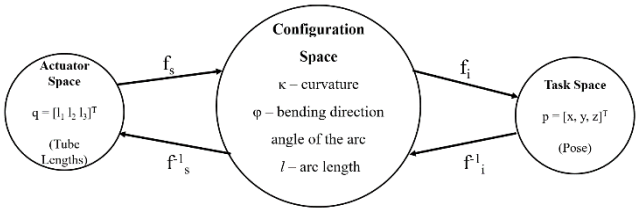

Fig. 1. Kinematic Mapping

In this mapping f_s indicates the robot specific mapping which pertains to the specific design of the robot while f_i indicates the robot independent mapping which can be formulated regardless of the design or type of soft robot.

A. Forward Kinematics

The robot independent mapping was derived. The robot was represented as a bendable cylinder with a backbone as shown in figure 2. In the figure, the z-axis was set pointing downwards to reflect the moving direction of the robot.

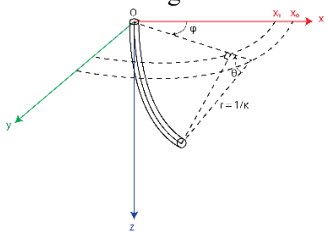

Fig. 2. Robot Coordinate System

φ is the angle the arc subtends between x and y axes, θ is the bending angle, r is the radius of curvature and κ is the curvature of the robot. The x-z plane is isolated by considering φ to be zero and deriving the end effector position p as shown in figure 3.

Thereby, considering the rotational transformations of θ about y-axis and φ about z-axis, the forward kinematic transformation matrix can be derived.

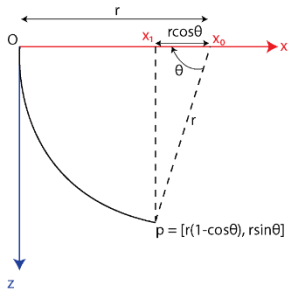

Fig. 3. Robot in Simplified X-Z Plane

$$p = [r(1-\cos\theta), 0, r\sin\theta]^T \quad (1)$$

$$f_i = T = \begin{bmatrix} R_z(\phi) & 0_{3\times1} \\ 0_{1\times3} & 1 \end{bmatrix} \begin{bmatrix} R_y(\theta) & p \\ 0_{1\times3} & 1 \end{bmatrix} \quad (2)$$

Further taking into account the formulae for curvature and arc length, the transformation matrix can be formulated,

$$\kappa = 1/r \quad (3)$$

$$\theta = s/r \qquad s \in [0, l] \quad (4)$$

The parameter s is a point along the arc and l is the length of the arc. Thereby, the x, y, and z equations can be extracted from the forward kinematic transformation matrix.

$$\begin{bmatrix} x \\ y \\ z \end{bmatrix} = \begin{bmatrix} \frac{\cos\phi\,(1-\cos\kappa s)}{\kappa} \\ \frac{\sin\phi\,(1-\cos\kappa s)}{\kappa} \\ \frac{\sin\kappa s}{\kappa} \end{bmatrix} \quad (5)$$

For the derivation of the robot independent mapping, the length of each actuator (l_1, l_2, l_3) along with the robot base geometry are taken into consideration.

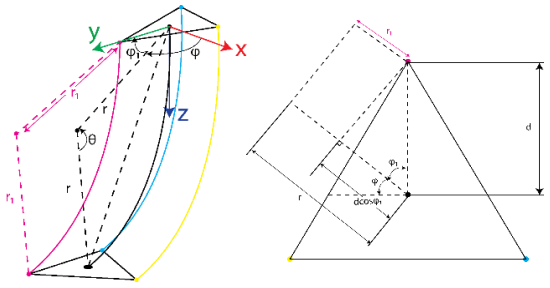

Fig. 4. Robot Actuator Lengths and Base Geometry

$$q = [l_1 \quad l_2 \quad l_3]^T \quad (6)$$

$$r_i = r - d\cos\phi_i \quad (7)$$

Considering equation 4, the length equation is obtained,

$$l = l_i + \theta d\cos\phi_i \quad (8)$$

Through substituting the values for φ_i (I = 1, 2, 3) and simplifying provides the length equation and φ equation with respect to the values of actuator lengths.

$$l(q) = \frac{l_1 + l_2 + l_3}{3} \quad (9)$$

$$\phi(q) = \tan^{-1}\left(\frac{\sqrt{3}(l_2 + l_3 - 2l_1)}{3(l_2 - l_3)}\right) \quad (10)$$

Considering the relationships in equation 3 and 4, the curvature equation can be derived with respect to the actuator length values.

$$\kappa(q) = \frac{2\sqrt{l_1^2 + l_2^2 + l_3^2 - l_1l_2 - l_1l_3 - l_2l_3}}{d(l_1 + l_2 + l_3)} \quad (11)$$

By utilizing equations 5, 9, 10, and 11, the forward kinematic can be analyzed using MATLAB 2020a as shown in figure 5. Varying the length values l_1, l_2 and l_3 provides the output of x, y, and z coordinates along with a graphical depiction of the robot backbone curvature.

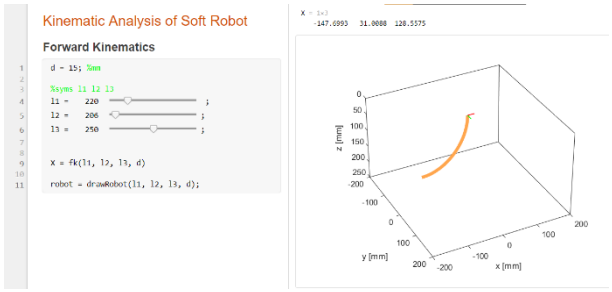

Fig. 5. Forward Kinematic Analysis

B. *Inverse Kinematics*

Using figures 2 and 3, the formulae for φ, κ and θ can be derived with respect to the x, y, and z positions.

$$\phi = \tan^{-1}\left(\frac{y}{x}\right) \quad (12)$$

$$\kappa = \frac{2\sqrt{x^2 + y^2}}{x^2 + y^2 + z^2} \quad (13)$$

$$\theta = \begin{cases} \cos^{-1}(1 - \kappa\sqrt{x^2 + y^2}), & z > 0 \\ 2\pi - \cos^{-1}\left(1 - \kappa\sqrt{x^2 + y^2}\right), & z \le 0 \end{cases} \quad (14)$$

Thereby, considering the length equation 8, the following parametric equation can be derived. The length for each actuator can be obtained through the substitution of equations 1_1,1_2 and 1_3 as well as setting I as 1, 2 or 3.

$$l_i = \frac{\theta}{\kappa} - \theta d\cos\left(\frac{2\pi}{3}(i-1) + \frac{\pi}{2} - \phi\right) \quad (15)$$

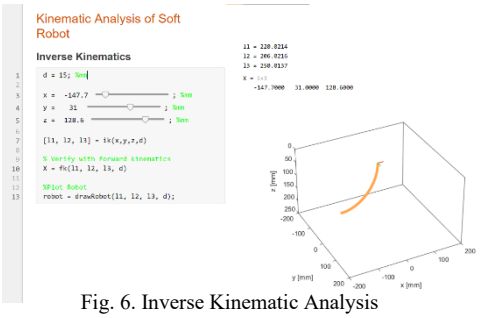

Fig. 6. Inverse Kinematic Analysis

Similar to the forward kinematics, the inverse kinematic simulation can be analyzed using MATLAB 2020a as shown in figure 6. Here, the position values for x, y, and z are provided and the length values l_1, l_2, and l_3 can be obtained. Feeding the result of the inverse kinematics provides the same

position input specified. This verifies the equations derived in this section.

III. HARDWARE

The design of this robot is based on the working principle of the Reverse Pneumatic Artificial Muscle (RPAM). The electronic circuit and pneumatic circuit was developed towards the control of the robot.

A. Mechanical Design

Figure 7 depicts the working principle of the RPAM design. The actuator tube is designed to be blocked on both ends with the top end having an air inlet. With the supply of air pressure, the tube expands in all directions similar to a balloon. However, the fiber reinforcement wrappings significantly limits the radial expansion, thus, allowing the actuator to only expand axially. This allows near linear extension of the actuator.

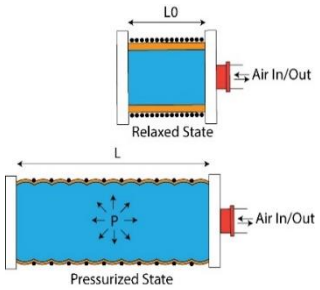

Fig. 7. Actuator Operating Principle

Figure 8 depicts the Solidwork design for the robot assembly including the gripper mechanism and frame. The actuators are designed to be stand-alone components with end caps. These end caps are designed to be assembled on to common plates that create the base and end effector.

Fig. 8. Full Assembly Design of Robot

B. Fabrication

The end caps, base, end effector, and gripper mechanism are 3D printed with PLA. The actuator is developed with a special technique in order to integrate the fiber reinforcements. This required 4 main components: latex rubber tubing, nylon fishing line, rubber cement and liquid latex rubber.

Figure 9 depicts the process to create the actuator. For the purpose of wrapping the fiber in a double helix pattern, a guide mold is designed and 3D printed. The mold is designed to be inserted and removed in parts, thus allowing safe demolding of the actuator. The end caps are coated with epoxy glue to avoid air leakage through the 3D print layer gaps. Furthermore, the end caps are glued to the actuator tube and hose clamps are used to pneumatically seal the actuators.

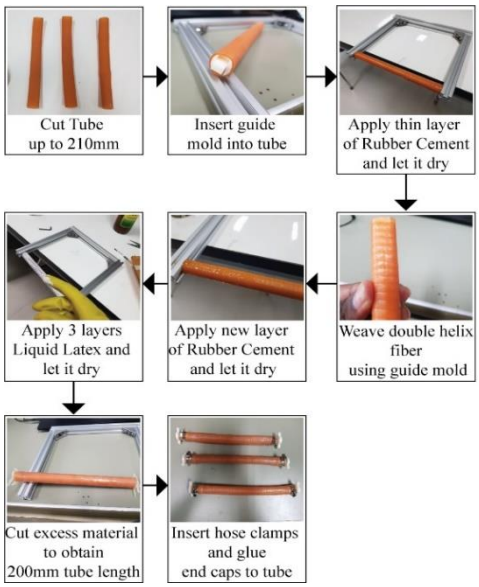

Fig. 9. Actuator Fabrication Flowchart

Each actuator weighs around 18g with length 200mm. After the fabrication process is complete, the actuator has a total wall thickness of 2.5mm. The amount of fiber wrapping turns were limited to 40 with 5mm spacing in between. Additional turns would provide added linearity due to further restriction of radial expansion. However, due to the manual fabrication method, higher number of wrapping turns was difficult to achieve.

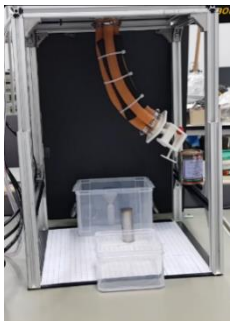

Fig. 10. Robot Assembly in action

The manipulator contains empty spaces in between each actuator. This causes a buckling effect when actuators are pressurized. Thereby, foam strips are inserted in between the actuators for support and cable ties are used to hold all the components together. Figure 10 depicts the assembly of the robot in action.

C. Pneumatic Circuit

The pneumatic circuit contains an air compressor, six 2/2 way solenoid valves, pneumatic speed controllers, three MPX5700DP pressure sensors and the fabricated actuators. Each actuator is pressurized with a fill valve and depressurized with an exhaust valve. The circuit is shown in figure 11.

D. Electronic Circuit

In addition to the solenoid valves and pressure sensors mentioned in the pneumatic circuit, potentiometers are used to provide manual setpoints, Arduino MEGA is used as the microcontroller and IRF520N MOSFET driver is used to interface the valve control signal with the 12V power supply.

An SG90 micro servo motor is used to actuate the gripper mechanism. The electronic circuit is shown in figure 12.

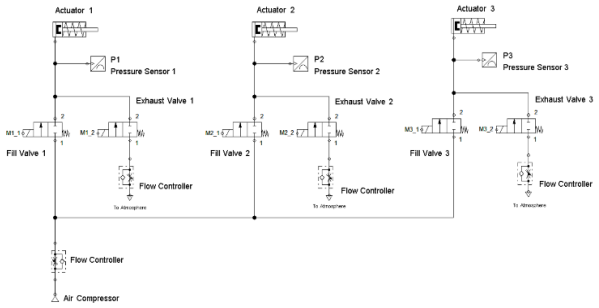

Fig. 11. Pneumatic Circuit

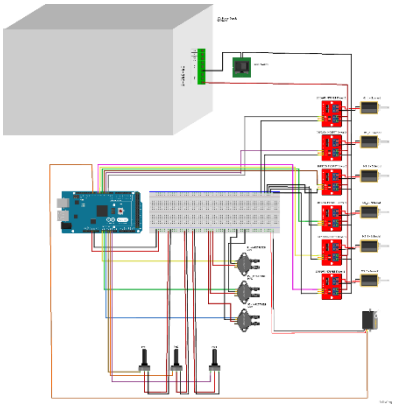

Fig. 12. Electronic Circuit

IV. Control Structure

The control of the robot is done in two stages. A state machine decides actuation profiles of the Fill and Exhaust valves with respect to the pressure conditions. PID control is used to regulate the pressure within the actuator. Due to the ON/OFF type solenoid valves utilized, pressure cannot be proportionally controlled. Thereby, the pressure is maintained within a dead-band of 10 kPa. Figure 13 depicts the state machine utilized in this research.

A. State Machine

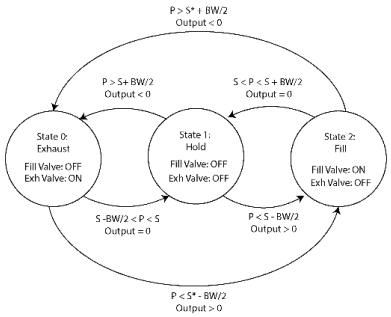

Fig. 13. State Machine

Where P is the pressure measurement, S is the setpoint provided, BW is the Dead-band Band Width (10 kPa) and S^* is the change in setpoint. The Exhaust State releases the pressure in the actuator while the Fill State increases the pressure. The Hold State blocks the pressure inside the actuator to maintain it within the defined dead-band. Due to small leakages, the pressure is constantly regulated in the Hold State. Therefore, the output of the actuator appears to oscillate within the Hold State.

B. PID Pressure Regulation

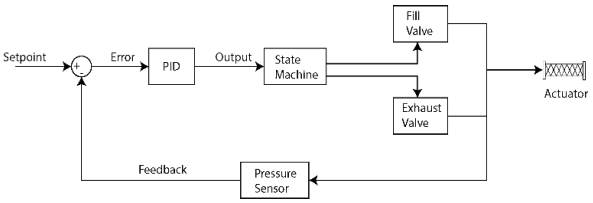

Fig. 14. PID Control

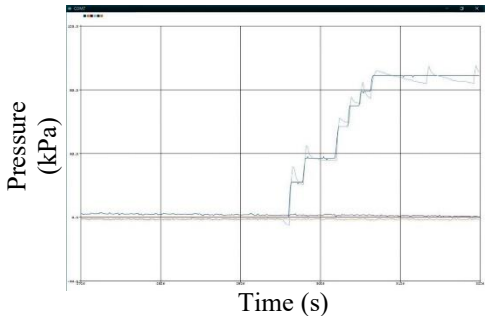

Fig. 15. Actuator Response for Step Changes

Based on the output of the PID control block, the State Machine decides to switch between the three states defined. Through empirical gain tuning, the best PID gains are selected as $k_p = 200$, $k_i = 5$, $k_d = 500$. High proportional and derivative gains cause detrimental results that make the system change from Fill and Exhaust States and cause undesirable oscillations. The integral term is not very effective due to the usage of the dead-band.

As observed in figure 15, when the potentiometer is used to change the pressure setpoint the pressure measurement follows the step changes. However, once the setpoint is set constant, i.e., Hold State, the drop in pressure causes the controller to regulate the pressure which results in an oscillatory movement. This scenario is unavoidable due to the hardware used in this research. Thereby, the PID tuning only provides smoother actuation for position control.

C. Position Control

The position control is conducted in two ways. Firstly, using the potentiometers to provide a manual pressure setpoint between 0-120 kPa which is used by the control system to regulate the pressure.The maximum limit is chosen to be 120 kPa as the pressures above 150 kPa causes the actuator to damage. With the dead-band limits the maximum pressure the actuators can safely reach is 125 kPa.

Secondly, a Look-Up Table (LUT) and interpolation is programmed to the code such that when a serial command is provided to the microcontroller, the position number is interpolated with the LUT and the relevant pressure combination is chosen as the setpoint. 26 position points are recorded reflecting on zero, half range (60 kPa) and full range (120 kPa) pressure combinations.

V. Experiments and Results

A. Look-Up Table

The setup is put through several experiments to verify that the robot is capable of operating within the proposed range. The LUT positions are recorded by providing the relevant

pressure setpoints and marking the x, y, and z coordinates on graph paper. Thereby, the data is processed to match the simulation configuration so that the recorded points and their simulation counterparts are compared as shown in figures 16 and 17. The robot successfully achieves a working environment of a hemispherical space of radius 12.37 cm and variation angle of 31°.

The resulting planes, the x, y and z values are averaged. From the results, the recorded positions are located in the same general direction and match with the simulated positions. However, there is an error in the recorded positions when compared to the simulated values as shown in figure 18. Error in the measurement, non-linearities in the material and actuation method causes the error.

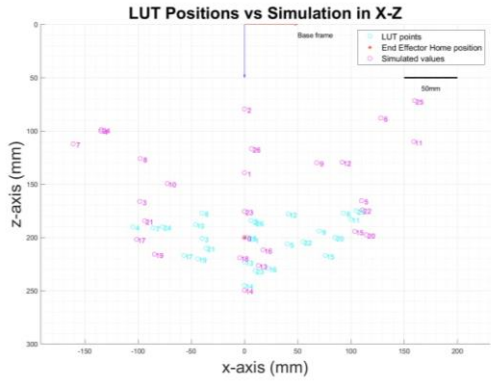

Fig. 16. Recorded Positions vs Simulations for X-Z plane

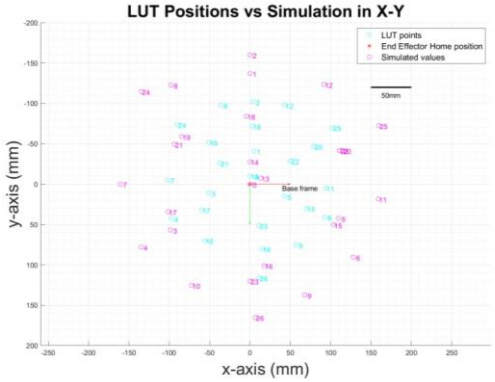

Fig. 17. Recorded Positions vs Simulations for X-Y plane

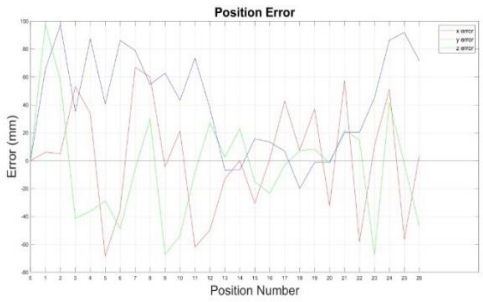

Fig. 18. Position Error

B. *Response Time*

Since Delta Robots are renowned for their fast actuation, the response time is investigated. Figure 21 shows the response time for a single actuator to achieve the relevant pressure. As expected higher pressures requires longer time to achieve. Figure 22 depicts the total response time consumed by the entire manipulator to achieve the desired position. The result reflects on the combination of pressures in each actuator.

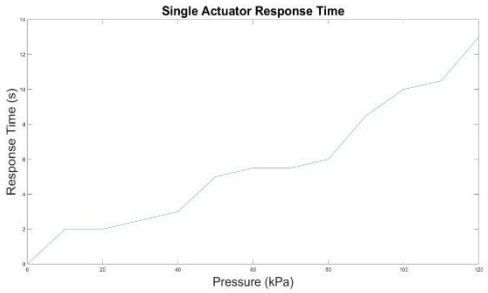

Fig. 21. Response of Single Actuator

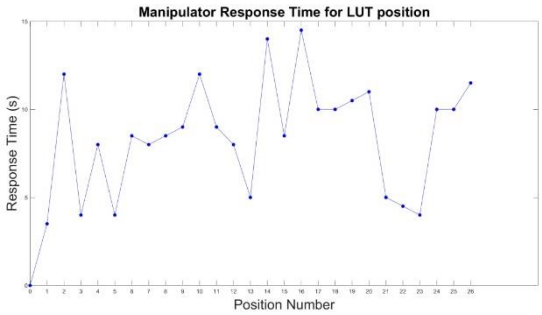

Fig. 22. Manipulator Response on LUT Positions

C. *Load Capacity*

Although the position control is effective in moving the robot based on the pre-defined position points and their interpolation, it is necessary to observe how the robot behaves when a payload is attached. Thereby, the error associated with the addition of weights can be depicted as in figures 23, 24 and 25 for x, y, and z respectively.

Adding more weight causes the error to increase. Positions with only one actuator pressurized have more error as the force output of the manipulator is not sufficient.

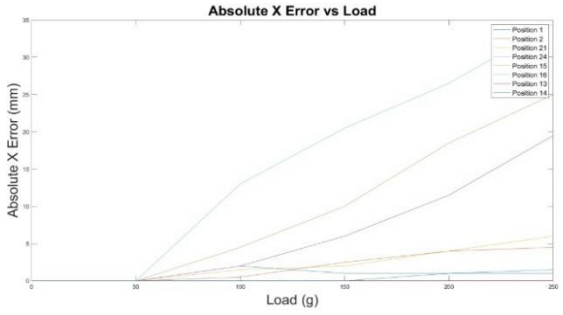

Fig. 23. Absolute Error in X Direction vs Load

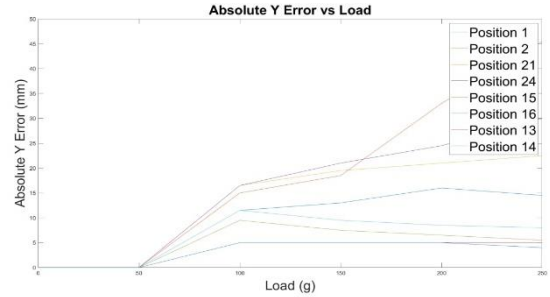

Fig. 24. Absolute Error in Y Direction vs Load

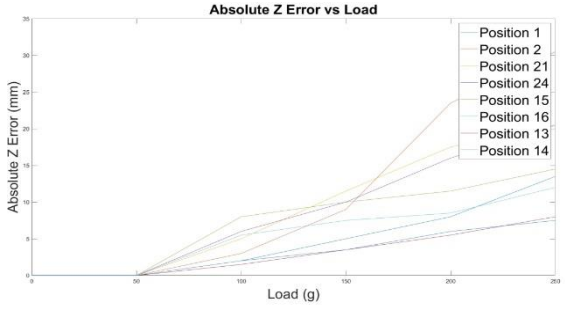

Fig. 25. Absolute Error in Z Direction vs Load

VI. Conclusion

In this paper we presented the kinematic model, design, fabrication and experimental results of a flexible actuation-based Delta Robot with the use of RPAM type actuator. Through testing and experimentation, the RPAM proved to be quite effective in extending its length without expanding radially. Thus, joining three RPAMs in a parallel configuration provided extending and bending motions to the robot.

The use of a fill and exhaust pair solenoid valve system to regulate pressure was challenging. Due to unavoidable leakages in the system, the system had to be controlled within a pressure dead-band, where the PID control system provided smoother actuation. The positioning of the robot was carried out by actuating individual tubes in certain sequences and the resulting positions were recorded on a Look-Up Table (LUT). The LUT was proved to be proficient in providing position control commands to the robot as per the user requirement.

We conducted the position control experiments and compared it with the simulated results from the constant curvature kinematic model. The comparison shows that the robot can be positioned towards the same simulated positions. However, it has to be noted that the error associated with the position is high. These inconsistencies may be due to the measurement errors and the non-linearities in materials and actuation methods used in this robot setup. The response time of the robot can be varied depending on the position and the pressure sequence of the actuators. However, the overall response time should be improved to achieve better Delta Robot-like behaviour. Since this robot system depends on flexible actuators, attaching payloads to the end effector causes the robot to deviate from its original LUT positions.

In conclusion, the Delta Robot developed in this study serves its purpose and can be considered an initial step in this area of flexible actuator-based robots. The RPAM type actuator is highly beneficial in achieving better reachability than the initial goal set for this research. However, the robot developed in this research has its shortcomings which can be improved upon in future work. The dynamic model, design and materials used can be improved to have better accuracies for position control while handling payloads with ease. The actuation response times could be improved through a better pressure regulation system hardware and control algorithm. Overall, the robot reachability could be improved through the use of multiple segments of parallel RPAM chains. We would like to investigate the effects of these improvements in future work in great detail.

References

[1] A. D. Marchese and D. Rus, “Design, kinematics (2016, June), and control of a soft spatial fluidic elastomer manipulator,” International Journal of Robotics Research, vol. 35, no. 7, pp. 840–869, doi: 10.1177/0278364915587925.

[2] G. Andrikopoulos, G. Nikolakopoulos, and S. Manesis (2013, December), “Pneumatic artificial muscles: A switching Model Predictive Control approach,” Control Engineering Practice, vol. 21, no. 12, pp. 1653–1664, doi: 10.1016/j.conengprac.2013.09.003.

[3] A. Hošovský, J. Piteľ, K. Židek, M. Tóthová, J. Sárosi, and L. Cveticanin (2016, September), “Dynamic characterization and simulation of two-link soft robot arm with pneumatic muscles,” Mechanism and Machine Theory, vol. 103, pp. 98–116, doi: 10.1016/j.mechmachtheory.2016.04.013.

[4] Skorina Erik H., S. O. Ming Luo, Fuchen Chen, Weijia Tao, and Cagdas D. Onal (2015), Feedforward augmented Sliding Mode Motion Control of Antagonistic Soft Pneumatic Actuators. Seattle, Washington: IEEE.

[5] E. H. Skorina et al. (2018, October), “Reverse pneumatic artificial muscles (rPAMs): Modeling, integration, and control,” PLoS ONE, vol. 13, no. 10, doi: 10.1371/journal.pone.0204637.

[6] E. W. Hawkes, D. L. Christensen, and A. M. Okamura (2016, June), “Design and implementation of a 300% strain soft artificial muscle,” in Proceedings - IEEE International Conference on Robotics and Automation, vol. 2016-June, pp. 4022–4029. doi: 10.1109/ICRA.2016.7487592.

[7] S. Habibian (2019), “Analysis and Control of Fiber-Reinforced Elastomeric Enclosures Analysis and Control of Fiber-Reinforced Elastomeric Enclosures (FREEs)”. [Online]. Available: https://digitalcommons.bucknell.edu/masters_theses

[8] J. W. Booth, J. C. Case, E. L. White, D. S. Shah, and R. Kramer-Bottiglio (2018, July), “An addressable pneumatic regulator for distributed control of soft robots,” in 2018 IEEE International Conference on Soft Robotics, RoboSoft 2018, pp. 25–30. doi: 10.1109/ROBOSOFT.2018.8404892.

[9] R. J. Webster and B. A. Jones (2010, November), “Design and kinematic modeling of constant curvature continuum robots: A review,” International Journal of Robotics Research, vol. 29, no. 13, pp. 1661–1683, doi: 10.1177/0278364910368147.